Published in final edited form as:
Neuroscience. 2008 June 23; 154(2): 595–605. doi:10.1016/j.neuroscience.2008.03.081.

Normal sleep homeostasis and lack of epilepsy phenotype in $GABA_A$ receptor α3 subunit-knockout mice

Raphaëlle Winsky-Sommerer[1], **Alana Knapman**[1], **Denise E. Fedele**[1], **Claude M. Schofield**[2], **Vladyslav V., Vyazovskiy**[1,3], **Uwe Rudolph**[4], **John R Huguenard**[2], **Jean-Marc Fritschy**[1], and **Irene Tobler**[1,*]

[1] *Institute of Pharmacology and Toxicology, University of Zurich, Zurich, Switzerland* [2] *Department of Neurology and Neurological Sciences, Stanford University Medical Center, Stanford, CA, USA* [4] *Laboratory of Genetic Neuropharmacology, McLean Hospital, Department of Psychiatry, Harvard, Medical School, Belmont, MA, USA*

Abstract

Thalamo-cortical networks generate specific patterns of oscillations during distinct vigilance states and epilepsy, well characterized by electroencephalography (EEG). Oscillations depend on recurrent synaptic loops, which are controlled by GABAergic transmission. In particular, $GABA_A$ receptors containing the α3 subunit are expressed predominantly in cortical layer VI and thalamic reticular nucleus (nRT) and regulate the activity and firing pattern of neurons in relay nuclei. Therefore, ablation of these receptors by gene targeting might profoundly affect thalamo-cortical oscillations. Here, we investigated the role of α3-$GABA_A$ receptors in regulating vigilance states and seizure activity by analyzing chronic EEG recordings in α3 subunit knockout (α3-KO) mice. The presence of postsynaptic α3-$GABA_A$ receptors/gephyrin clusters in the nRT and $GABA_A$-mediated synaptic currents in acute thalamic slices were also examined.

EEG spectral analysis showed no difference between genotypes during non rapid-eye movement (NREM) sleep or at waking-NREM sleep transitions. EEG power in the spindle frequency range (10–15 Hz) was significantly lower at NREM-REM sleep transitions in mutant compared to wild-type mice. Enhancement of sleep pressure by 6 h sleep deprivation did not reveal any differences in the regulation of EEG activities between genotypes. Finally, the waking EEG showed a slightly larger power in the 11–13-Hz band in α3-KO mice. However, neither behavior nor the waking EEG showed alterations suggestive of absence seizures. Furthermore, α3-KO mice did not differ in seizure susceptibility in a model of temporal lobe epilepsy. Strikingly, despite the disruption of postsynaptic gephyrin clusters, whole-cell patch clamp recordings revealed intact inhibitory synaptic transmission in the nRT of α3-KO mice. These findings show that the lack of α3-$GABA_A$ receptors is extensively compensated for to preserve the integrity of thalamo-cortical function in physiological and pathophysiological situations.

*Corresponding author: Institute of Pharmacology and Toxicology, University of Zurich, Winterthurerstrasse 190, CH-8057 Zurich, Switzerland., Phone: +41 44 635 59 57, Fax: +41 44 635 57 07, Email address: tobler@pharma.uzh.ch.
[3]Present address: Department of Psychiatry, University of Wisconsin, Madison, WI, USA

Section Editor: Werner Sieghart

Keywords

Thalamo-cortical network; EEG rhythms; spectral analysis; gephyrin; spike-wave discharges; sleep deprivation

Changes in brain electrical activity during vigilance states and epilepsy are evidenced by complex rhythms in the electroencephalogram (EEG). Frequency, amplitude and modulation of neuronal oscillations are determined by the firing patterns and connectivity of specific neuronal networks (Llinas and Steriade, 2006). In particular, the functional coupling of the thalamus and cerebral cortex plays a strategic role in the emergence of behaviorally relevant rhythmic activities (Steriade et al., 1993) and hypersynchronization leading to seizures (Timofeev and Steriade, 2004). The function of thalamo-cortical circuits depends critically on reciprocal synaptic loops between thalamic relay nuclei, the thalamic reticular nucleus (nRT) and the neocortex (Jones, 2002, Pinault, 2004). These reciprocal excitatory and inhibitory connections, as well as inputs to this network, give rise to specific oscillatory activities that underlie EEG rhythms (Domich et al., 1986, Steriade et al., 1986, Steriade, 2003).

The nRT, exclusively composed of GABAergic neurons, plays a pivotal role in oscillatory activities by providing a powerful and widespread inhibitory tone onto thalamic relay nuclei (Huguenard and Prince, 1994b, Cox et al., 1996). The activity of nRT neurons is, in turn, modulated by afferent fibers from several brain regions including thalamic nuclei, brainstem and basal nuclei, and the most powerful input connections arise from cortical layer VI (Liu and Jones, 1999). Importantly, nRT neurons are interconnected via GABAergic synapses (Jones, 2002). $GABA_A$ receptor-mediated currents in both the nRT and relay thalamic nuclei are critical in modulating neuronal firing patterns in thalamo-cortical circuits (von Krosigk et al., 1993, Cox et al., 1997).

These integrated recurrent synaptic loops enable the synchronized neuronal activity underlying major EEG rhythms, notably delta waves, spindles, and the cortical slow oscillation, which define non-rapid-eye movement (NREM) sleep (Steriade, 2006). In contrast, abnormal activity of the thalamo-cortical network can lead for example, to the onset of spike-wave discharges that are EEG hallmarks of absence seizure episodes (for review, Steriade, 2003, Steriade, 2005). Numerous studies have demonstrated the importance of nRT neurons in network desynchronization, which prevents widespread activity and subsequent hypersynchrony leading to seizures (Steriade et al., 1993, von Krosigk et al., 1993, Huguenard and Prince, 1994a, Huntsman et al., 1999, Sohal et al., 2000, Sohal and Huguenard, 2003, Sohal et al., 2003).

The functional and pharmacological properties of $GABA_A$ receptors depend on their subunit composition. A large family of constituent subunits (α1–6, β1–3, γ 1–3, δ, ρ1–3, θ, π,ε) allows the assembly of a variety of $GABA_A$ receptor subtypes (Rudolph and Mohler, 2006). Strikingly, the nRT mainly expresses $GABA_A$ receptors containing the α3 subunit (α3-$GABA_A$ receptors) (Wisden et al., 1988, Wisden et al., 1992, Fritschy and Mohler, 1995, Pirker et al., 2000, Studer et al., 2006) and this receptor subtype is also abundant in layer VI of the neocortex. Although when assayed in whole brain this subtype represents a minor subpopulation of $GABA_A$ receptors (10–15%), it is predominant in several neuronal networks (i.e., arousal activating systems as well as sleep-promoting circuitries) that play a key role in the generation and maintenance of the sleep-wake cycle (Gao et al., 1993, Fritschy and Mohler, 1995, Gao et al., 1995, Rodriguez-Pallares et al., 2001, Jones, 2005).

In α3-KO mice, there is no detectable change in the expression of other α subunit variants (Yee et al., 2005) and no replacement ofα3-$GABA_A$ receptors in the nRT by another subtype

is apparent (Studer et al., 2006). Therefore, we hypothesized that changes in neuronal activity in the nRT and neocortical layer VI due to lack of α3-$GABA_A$ receptors may alter thalamo-cortical activity and thereby result in a sleep phenotype or enhanced susceptibility to epileptic seizures. A recent study has shown that genetically epilepsy-prone rats, displaying abnormal thalamic synchronization, exhibit a specific loss of α3-$GABA_A$ receptors in the nRT (Liu et al., 2007). Here, we performed chronic EEG recordings in freely moving wild-type (WT) and α3-KO mice to investigate alterations in sleep and wakefulness and test for the presence of spike-and-wave discharges. Next, we studied the response of α3-KO mice to sleep deprivation (SD), a well-established method to enhance sleep pressure and thereby uncover differences in sleep regulation. Finally, the susceptibility of α3-KO mice to experimentally-induced recurrent focal seizures was investigated in a model of temporal lobe epilepsy (TLE). To further assess potential alterations of inhibitory synaptic transmission in the nRT, we performed whole-cell patch clamp recordings on thalamic slices obtained from juvenileα3-KO mice and investigated gephyrin and α3-$GABA_A$ receptor clustering at postsynaptic sites in the nRT using immunofluorescence staining.

Experimental procedures

Animals

Mice lacking the $GABA_A$ receptor α3 subunit (α3-KO) and their WT controls were maintained on either 129X1/SvJ or C57Bl/6J background (see Yee et al., 2005 for characterization) and genotyped by PCR analysis of tail biopsies. Mice were housed individually with *ad libitum* access to food and water. The animal facility was maintained on a 12 h light-dark cycle (light on at 9 am; ~ 30 lux), at a constant ambient temperature (22–24°C) and 50 % relative humidity. All experimental procedures were carried out in accordance with the European Communities' Council Directive of 24 November 1986 (86/609/EEC) and were approved by the Cantonal Veterinary Office of Zurich or the Stanford University Institutional Animal Care and Use Committee.

Sleep and motor activity recordings

Surgery—A first group of adult 129X1/SvJ mice (male) was used for surgery (11–13 weeks-old at surgery; α3-KO: n=12, 35.8 ± 2.0 g; WT: n=11, 31.2 ± 1.4 g). For EEG recording, mice were implanted epidurally under deep anesthesia (ketamine 100 mg/kg - xylazine 20 mg/kg, 10 ml/kg, i.p.). Gold-plated miniature screws (diameter 0.9 mm) were positioned on the right hemisphere above the frontal cortex (1.5 mm anterior to bregma and 2 mm lateral to the midline) and the parietal cortex (2 mm posterior to bregma and 3 mm lateral to the midline). A reference electrode was placed above the cerebellum (2 mm posterior to lambda, on the midline). Electrodes were connected to stainless steel wires and fixed to the skull with dental cement. Two gold wires (diameter 0.2 mm) were inserted bilaterally in the neck muscles to record the electromyogram (EMG). After 3 weeks recovery, the mice were adapted for at least 3 days to the recording conditions.

EEG recording—Continuous EEG-EMG recordings were obtained throughout 48 h. A 24-h baseline recording was followed by 6 h sleep deprivation (SD) starting at light onset, and the subsequent 18 h recovery. SD was performed by introducing a variety of objects (e.g. nesting material, pieces of wood) into the cage, as well as by gently tapping on the cage whenever a mouse appeared to be drowsy (Tobler et al., 1997). The mice were under constant observation and motor activity was continuously recorded by an infra-red (IR) sensor placed above the cage during the two experimental days.

Data acquisition and analysis—The EEG and EMG signals were amplified (amplification factor approx. 2000), conditioned by analogue filters (high-pass filter: −3dB at 0.016 Hz; low-

pass filter: −3 dB at 40 Hz, less than −35 dB at 128 Hz.) sampled with 256 Hz, digitally filtered (EEG: low-pass FIR filter 25 Hz; EMG: band-pass FIR 20–50 Hz) and stored with a resolution of 128 Hz. EEG power spectra were computed for consecutive 4-s epochs by a Fast Fourier Transform routine within the frequency range of 0.25–25 Hz. Between 0.25 and 5 Hz, the 0.25 Hz bins were added to yield 0.5 Hz bins, and between 5.25 and 25 Hz to yield 1 Hz bins.

Based on the raw parietal and frontal EEG, the corresponding slow-wave activity (SWA), as well as the raw and integrated EMG, three vigilance states were visually scored for 4-s epochs as NREM sleep, rapid-eye movement (REM) sleep and waking (Tobler et al., 1997). Epochs containing artifacts were identified and excluded from spectral analysis (% of recording time: α3-KO: 7.5 ± 1.7; WT: 6.4 ± 2.3%). Data analysis was carried out using the MATLAB software package (The Math Works, Inc., Natick, MA, USA).

Motor activity—Motor activity was also recorded in a second group of mice (~12 weeks-old; male; n=9 α3-KO mice; n=10 WT). These mice did not undergo EEG-EMG surgery and were littermates of the mice included in the sleep experiment. After at least 10 days adaptation, motor activity was recorded continuously for 10 days via an IR sensor placed above the cage. Activity counts were stored in 1-min epochs (Tobler et al., 1996) and 10-day mean activity profiles were computed (Stanford Software Systems, Chronobiology Kit). Rest was defined as the amount of 1-min epochs where activity counts equaled zero.

Statistics—One-way ANOVA factor ‘genotype’ was used to compare baseline spectra (0.25–25 Hz) during the 12-h light period of the baseline between WT and α3-KO mice. When significance was reached, *post-hoc* unpaired *t*-tests were performed. The EEG spectra at transitions were computed for a specific frequency band (i.e., spindle range: 10–15 Hz; SWA: 0.75–4 Hz) as a percentage of the corresponding mean power in the same band in NREM sleep during the 12-h baseline light period. Two-way ANOVA with factors ‘genotype’ and ‘epoch’ was used followed by a *post-hoc* unpaired *t*-test when significance was reached. All analyses of sleep are based on the 24-h baseline and 6-h recovery after SD. The NREM sleep and REM sleep spectra for the two hours following SD were expressed as a percentage of the corresponding baseline hour of each individual animal. Means were thereafter computed for each genotype. Frequency bins from 0.25–25 Hz were compared using a one-way ANOVA with factor ‘genotype’ followed by unpaired *t*-tests when significance was reached. The time course of slow-wave activity following SD was subjected to a one-way ANOVA factor ‘genotype’ to compare genotypes. To compare the amount of activity and rest in the two genotypes, an unpaired *t*-test was used. Vigilance states during baseline and recovery from SD were compared between genotypes by unpaired *t*-test. For statistical analysis SAS (SAS Institute, Inc., Cary, NC, USA) was used. Statistical significance was set at $p<0.05$.

Induction of Temporal Lobe Epilepsy (TLE) model

Kainic acid injection—Under isoflurane general anesthesia, WT (n=13) and α3-KO (n=14) C57BL/6J mice received a unilateral stereotaxic injection of 50 nl of a 20 mM solution of kainic acid (Calbiochem; San Diego, CA) in saline (i.e., 1 nmol kainic acid) into the right CA1 area of the dorsal hippocampus (coordinates with bregma as reference: anteroposterior = −1.7 mm, mediolateral = −1.6 mm, dorsoventral = −1.9 mm) as described (Kralic et al., 2005).

Electrode implantation and EEG recording—Spontaneous recurrent focal seizures in kainic acid-treated mice were recorded by EEG at 14 and 28 days post-injection. Sixteen mice were implanted immediately following kainic acid injection with a bipolar electrode inserted into the right hippocampus at the same coordinates as for kainic acid injection and a monopolar reference electrode placed over the cerebellum, as described (Kralic et al., 2005). The electrodes were fixed to the skull with cyanoacrylate and dental cement. EEG activities were

recorded in freely moving animals placed in a Faraday cage using a digital acquisition computer-based system (MP100WSW System; Biopac Systems, Inc., Santa Barbara, CA; six channels, sampling rate 200 Hz). Before beginning EEG recordings, mice were habituated for 1 h to the test cage. At the end of the last recording session, mice were sacrificed by perfusion-fixation and brain sections processed for Cresyl violet staining to assess the effects of kainic acid on the cytoarchitecture of the hippocampus and the location of electrodes. A separate group of WT and α3-KO mice was not implanted with electrodes and analyzed histologically at 10, 14, and 28 days post-kainate injection.

Immunofluorescence staining

WT andα3-KO C57BL/6J male mice aged P14-P15 (n=11) were deeply anesthetized with Nembutal (50 mg/kg, i.p.) and perfused through the ascending aorta with 4% paraformaldehyde in 0.15 M phosphate buffer (pH 7.4). Brains were postfixed overnight, cryoprotected in sucrose, frozen and cut either transversally or parasagitally at 40 μm with a sliding microtome. Sections were collected in PBS and stored in an antifreeze solution (15% glucose and 30% ethylene glycol in 50 mM phosphate buffer, pH 7.4) prior to use.

To enhance the detection of postsynaptic proteins, free-floating sections were incubated for 15 min at 37ºC in 0.15 mg/ml pepsin diluted in 0.2 M HCl (Watanabe et al., 1998). They were then rinsed with Tris buffer and incubated overnight at 4°C with a mixture of primary antibodies against the $GABA_A$ receptor α3 subunit (Fritschy and Mohler, 1995), gephyrin (mAb7a, Synaptic Systems, Göttingen, Germany), and vesicular amino acid transporter (VIAAT, Synaptic Systems) diluted in Tris buffer containing 2% normal goat serum and 0.2% Triton X-100. Sections were then washed and incubated for 30 minutes at room temperature in secondary antibodies (anti-guinea pig, anti-mouse, and anti-rabbit) conjugated with different fluorochromes (Alexa488, Molecular Probes, Eugene, OR; Cy3 and Cy5, Jackson Immunoresearch, West Grove, PA). Sections were then washed again, mounted on gelatin-coated slides, air-dried and coverslipped with fluorescence mounting medium (Dako, Glostrup, Denmark). Sections from WT and mutant mice were processed in parallel under identical conditions to minimize variability in staining intensity.

Ex-vivo electrophysiology

Thalamic slices were obtained from WT andα3-KO C57BL/6J mice (n=8 and n=6 mice respectively; postnatal days P12–P15; either gender). Mice were anesthetized with pentobarbital and decapitated. The brain was rapidly removed and transferred into ice-cold solution containing (in mM): 234 sucrose, 11 glucose, 24 $NaHCO_3$, 2.5 KCl, 1.25 NaH_2PO_4, 10 $MgSO_4$, and 0.5 $CaCl_2$, equilibrated with 95% O_2/5% CO_2. Horizontal slices (275–300 μm thickness) containing the ventrobasal thalamus and adjacent nRT were obtained with a vibratome. Thalamic slices were transferred into a chamber with artificial cerebral spinal fluid (ACSF) containing (in mM): 126 NaCl, 26 $NaHCO_3$, 2.5 KCl, 1.25 NaH_2PO_4, 2 $MgCl_2$, 2 $CaCl_2$, and 10 glucose, equilibrated with 95% O_2/5% CO_2 and incubated at 33°C for at least 1 h, then brought to room temperature before recording.

Recordings were made at room temperature (22–24°C) using whole-cell patch-clamp methodology. Following incubation, thalamic slices were transferred to the recording chamber, and held in place by a nylon grid while continuously superfused with ACSF at a flow rate of 2 ml/min. Thalamic neurons in the nRT were visually identified (Huntsman et al., 1999) using a fixed-stage upright microscope (Axioskop, Zeiss, Thornwood, NY) equipped with an insulated 63x objective and Nomarski DIC optics. Recordings were performed under voltage-clamp at −60 mV using a MultiClamp 700A amplifier (Molecular Devices, Sunnyvale, CA). Recording electrodes were made of borosilicate glass and had a resistance of 1.8–2.8 MΩ when filled with intracellular solution, which contained (in mM): 135 CsCl, 10 HEPES, 10 EGTA,

5 QX-314, 5 ATP-Mg^{2+}; pH was 7.3 and osmolarity was adjusted to 300 mOsm with sucrose. During recordings, spontaneous inhibitory postsynaptic currents (sIPSCs) were pharmacologically isolated by bath application of the ionotropic glutamate receptor blockers 6,7-Dinitro-quinoxaline-2,3-dione (DNQX, 20 μm, Sigma, St. Louis, MO) and 2-Amino-5-phosphonopentanoic acid (AP-5, 100 μm, Tocris Biosciences, Ellisville, MO). The $GABA_A$ receptor antagonists SR-95531 (20 μM) and bicuculline (50 μM) (Sigma, St. Louis, MO, USA) were applied to abolish sIPSCs. The effect of the high affinity $GABA_C$ antagonist TPMPA ((1,2,5,6-Tetrahydropyridin-4-yl)-methylphosphinic acid; 50 μM) was also assessed. Access resistance was monitored and cells were included for analysis only if the series resistance was <15 MΩ and the change of resistance was <25% over the course of the experiment. Data were acquired in gap free mode at 10 kHz using pClamp 9 (Molecular Devices) and filtered at 2 kHz. Custom software (Detector, WinScanSelect, J.R. Huguenard) were used to detect, sort, and measure sIPSCs. At least n=50 isolated IPSCs per cell were aligned and averaged to give the mean response for each cell.

Results

Unaltered EEG rhythms and sleep regulation in adult α3-KO mice

Baseline EEG power spectra—We performed spectral analysis and compared EEG power density in the three vigilance states (i.e., waking, NREM sleep and REM sleep) during the baseline 12-h light period between genotypes. In α3-KO mice, the waking EEG spectra exhibited higher values compared to the WT controls in frequencies encompassing the spindle range (11–13 Hz) as well as at 22–23 Hz (Fig. 1; one-way ANOVA factor 'genotype', $p< 0.05$ *post-hoc* unpaired *t*-test). These changes were specific to the frontal derivation. The NREM sleep EEG showed no difference between genotypes in either derivation (Fig. 1). Total EEG power (0.75–25 Hz) in NREM sleep did not differ significantly between the two genotypes (μV^2, frontal derivation: α3-KO 4103 ± 251, WT 4247 ± 395; parietal derivation: α3-KO 6485 ± 352, WT 7234 ± 623; unpaired *t*-test p=0.76 and 0.32, respectively).

To further analyze the difference in the waking EEG spectra within the spindle frequency range, we computed EEG power for the 10–15 Hz frequency band one minute before and after the waking-NREM sleep transitions (Fig. 2A). Two-way ANOVA (factors 'genotype' and '12-s epoch') revealed a significant difference between α3-KO mice and WT (p=0.04), corresponding to the increase in EEG power observed above. However, the interaction 'genotype' × '12-s epoch' did not reach significance (p=0.35).

Previous studies have shown that, in some mouse strains, spindles are observed mainly in the frontal derivation and are found predominantly in NREM sleep, as well as immediately before the transition between NREM sleep and REM sleep (Valatx and Bugat, 1974, Vyazovskiy et al., 2004). Therefore, we also computed EEG power (10–15 Hz) one min before and after transitions between NREM sleep and REM sleep (Fig. 2B). The α3-KO mice did not show the typical surge in power at the spindle frequency range immediately before the transition from NREM sleep to REM sleep while WT mice showed a significant power surge in the last 12-s epoch before the transition ($p<0.05$, *post-hoc* unpaired *t*-test when significance was reached after a two-way ANOVA factors 'genotype' × 'epoch'). Since the nRT gates the transitions from wake to sleep (Steriade et al., 1993, Pinault, 2004), we investigated SWA at these transitions. No differences occurred between the genotypes (Fig. 2C).

Effects of sleep deprivation on sleep EEG power density—To investigate whether the genotypes differ when challenged by enhancing their sleep pressure, we analyzed the sleep EEG after 6 h SD. In the first 2 h recovery after SD, a significant increase in EEG power in NREM sleep was observed for broad frequency ranges encompassing SWA (0.75–4 Hz) and spindles (10–15 Hz) in both the frontal and parietal derivations (Fig. 3). No significant

differences occurred between genotypes during these first 2 h recovery, except in high frequencies between 21–25 Hz in the parietal derivation (one-way ANOVA factor 'genotype' followed by unpaired *t*-test, $p<0.05$).

Time course of slow-wave activity during baseline and recovery after SD—To further investigate the effects of SD on NREM sleep, we computed SWA, an index of sleep intensity (Borbély and Achermann, 2005). Previous reports have shown that the slow and high SWA frequencies do not have an identical time course (Huber et al., 2000b). Thus, we also subdivided SWA into a low and a high frequency band (0.75–2.5 Hz and 2.75–4 Hz, respectively). No differences were observed between genotypes in the time course of SWA in these two bands (not shown). As expected, SD induced a significant increase in SWA during recovery in both frequency bands, in both genotypes and derivations, compared to the corresponding baseline values ($p<0.05$ *post-hoc* paired *t*-test when significance was reached after rANOVA with factors 'day' and 'interval').

Effect of α3 subunit gene deletion on REM sleep—The α3-$GABA_A$ receptor is the main subtype expressed in neuronal populations involved in the regulation of REM sleep (basal forebrain cholinergic neurons, as well as brainstem monoaminergic and serotonergic neurons). Thus, we investigated whether the deletion of the α3 subunit affects REM sleep. In α3-KO mice, REM sleep power density showed higher values in the 0.5–1 Hz bin and in frequencies between 4–6 Hz, in the frontal and parietal derivation respectively (Fig. 1. $p< 0.05$ *post-hoc* unpaired *t*-test when significance was reached for one-way ANOVA factor 'genotype'). Theta rhythms (4–9 Hz) characterize the EEG during REM sleep and exploratory behavior. A finer analysis showed a faster theta-peak frequency in the parietal derivation inα3-KO mice (α3-KO: 6.31 ± 0.03 Hz *versus* WT: 6.11 ± 0.05 Hz; unpaired *t*-test $p=0.0034$). This difference was no longer observed during recovery after 6 h SD (α3-KO: 6.36 ± 0.07 Hz *versus* WT: 6.46 ± 0.03 Hz; unpaired *t*-test $p=0.2111$). Next, we investigated whether increased sleep pressure leads to differences in the REM sleep EEG. We found that EEG power in REM sleep showed several minor alterations in the first 2 hours of recovery following SD in both genotypes and derivations (Fig. 3). The α3-KO mice displayed significantly higher values in EEG power in the frequency bins including the spindle frequency range (10–12 Hz and 11–13 Hz in the frontal and parietal derivation respectively) compared to WT control mice (Fig. 3; one-way ANOVA 'genotype' followed by unpaired *t*-test $p< 0.05$). These differences were no longer present during the subsequent hours of recovery (data not shown). Furthermore, the number of REM sleep episodes lasting between 28–60 s were slightly but significantly more abundant in α3-KO mice compared to WT mice (data not shown).

Baseline vigilance states and effect of sleep deprivation—The amount of time spent in each of the three vigilance states, waking, NREM sleep, and REM sleep was compared during baseline and during recovery after 6 h SD. No differences were found between genotypes in the baseline values (Table 1), and the effects of SD on these vigilance states were similar in both genotypes (Table 1; unpaired *t*-test showed no significant difference).

Motor activity—Since exploratory behavior during wakefulness affects the EEG spectrum during subsequent sleep (Huber et al., 2007), we assessed whether deletion of the α3 subunit gene results in alterations of motor activity in a familiar environment (i.e., home cage). No differences were observed between genotypes in intensity of activity (24-h values; mean counts/active epoch ± SEM: α3-KO: 8.9 ± 0.3 (n=9) *vs* WT: 9.6 ± 0.3 (n=10); unpaired *t*-test comparing 10-day means) or in the amount of rest (24-h values, min ± SEM: α3-KO: 1157.6 ± 15.0 *vs* WT: 1205.3 ± 17.5; unpaired *t*-test comparing 10-day means).

Lack of spontaneous spike-wave discharge patterns in mutant mice—The lack of α3-$GABA_A$ receptors in the nRT and cortical layer VI may affect the tight control that prevents hypersynchrony underlying slow-wave discharges, a hallmark of epileptic seizures. Moreover, abnormalities in the EEG patterns of mutant mice may in particular be detected at the transitions between vigilance states when changes of activity take place in thalamic neurons. Finally, our SD paradigm may facilitate seizure episodes in mutant mice. However, visual inspection of raw EEG traces during waking and NREM sleep, under baseline conditions or during SD, as well as at transitions between vigilance states, did not provide any evidence of abnormalities such as spike-wave discharges in α3-KO mice. Furthermore, behavioral monitoring during SD did not reveal any abnormalities in mutant mice.

Unaltered epilepsy phenotype in adult α3-KO mice—To determine whether α3-$GABA_A$ receptors in thalamo-cortical circuits contribute to the regulation of seizures and epileptogenesis and to assess the vulnerability of α3-KO mice to an excitotoxic insult, we investigated these mutant mice and WT controls in a model of TLE induced by a unilateral intrahippocampal injection of kainic acid. Chronic recurrent seizures were detected by EEG recordings performed at 14 and 28 days post-kainate injection in 12 mice, whereas histological alterations induced by kainic acid were assessed by Nissl staining after 10, 14, and 28 days in a total of 13 WT and 14 mutant mice.

EEG recordings revealed abnormal neuronal activity patterns, with frequent, irregular spikes at 14 days post-kainate injection, without difference between genotypes. Chronic recurrent seizures recorded two weeks later (28 days post-kainate) also were similar in WT and mutant mice (Fig. 4A), both in terms of frequency and duration of seizures (defined here as ictal events lasting more than 10 sec). Likewise, the frequency of short ictal events (1–10 sec) was unchanged. Examination of Nissl-stained sections revealed comparable histological alterations after kainate treatment in both genotypes, with extensive neurodegeneration occurring between day 10 and day 28. At the latter stage, the injected side was characterized by extensive loss of pyramidal cells in CA1 and CA3, as well as hilar cells, and a prominent dispersion of dentate gyrus granule cells (Fig. 4B–C). These features are typical for this model of TLE (Bouilleret et al., 2000).

Alteration of gephyrin and $GABA_A$ receptor clustering in nRT neurons of juvenile α3-KO mice—We have reported previously that gephyrin and $GABA_A$ receptor clustering at postsynaptic sites of nRT neurons is altered in adult α3-KO mice (Studer et al., 2006). To determine whether this deficit occurs secondarily due to a failure to maintain GABAergic synapses formed during ontogeny or whether synapse formation is impaired in these mutant mice, the analysis was performed in juvenile mice (P15), during the peak of synaptogenesis. Triple immunofluorescence staining for the α3 subunit, gephyrin, and VGAT revealed a normal distribution of GABAergic terminals in the nRT from both genotypes. However, while gephyrin clusters colocalized with $GABA_A$ receptor subunit staining were readily evident in WT mice, no such clusters were seen in α3-KO mutants (Fig. 5A–B). Staining for the α3 subunit was not detectable, whereas a few gephyrin aggregates were visible, but were not associated with VIAAT-positive terminals. Similar aggregates, but of larger size, have been reported in nRT neurons of adult mice (Studer et al., 2006). These results strongly suggest that the α3 subunit is required for the formation of postsynaptic $GABA_A$ receptor and gephyrin clusters, but does not affect the morphology or distribution of GABAergic terminals in the nRT. This effect of the mutation was cell-specific, as gephyrin clustering was intact in neighboring regions that mainly express other $GABA_A$ receptor subtypes (striatum, globus pallidus, hippocampal formation; not shown).

***Ex-vivo* electrophysiology in juvenile α3-KO mice—**In view of the surprisingly minor differences in the sleep EEG between α3-KO mice and WT mice, we assessed the impact of

α3 subunit gene deletion on inhibitory neurotransmission by performing whole-cell patch clamp recordings in nRT neurons of juvenile α3-KO mice and their WT controls. Similar to WT mice, spontaneous IPSCs were robustly detected in the nRT of α3-KO mice (Fig. 5C). Bath application of the specific $GABA_A$ receptor antagonists SR-95531 (8 cells from α3-KO mice), as well as bicuculline, completely abolished sIPSCs (5 cells fromα3-KO mice), demonstrating that these events are $GABA_A$ receptor-mediated. Moreover, IPSCs remained intact after bath application of the high affinity $GABA_C$ antagonist TPMPA, providing evidence that they are not mediated by $GABA_C$ receptors (4 cells from α3-KO mice). We analyzed the mean IPSC response averaged from WT (10 cells from 8 mice) and α3-KO (10 cells from 6 mice) nRT neurons (Fig. 5D–E). Events from α3-KO mice were significantly larger in amplitude compared to WT mice (WT = −20 ± 2 pA *versus* α3-KO = −55 ± 5 pA, unpaired *t*-test), while the frequency of events was slightly increased, though not significantly, in α3-KO mice (WT = 2.0 ± 0.2 Hz; α3-KO = 2.6 ± 0.3 Hz).

Discussion

Given the restricted expression of theα3-$GABA_A$ receptors in neuronal populations playing a key role in the generation of brain rhythms, we expected to observe an unambiguous behavioral phenotype in α3-KO mice. Indeed, the lack ofα3-$GABA_A$ receptors should induce changes in the intrinsic firing of the nRT and cortical layer VI neurons, and subsequently alter the activity of the thalamo-cortical circuits. Paradoxically, α3-KO mice did not show any major deficiencies in their sleep regulation or epilepsy phenotype (Fig. 1–4), suggesting potent "rescue" mechanisms to stabilize the activity of thalamo-cortical networks in the absence of the main $GABA_A$ receptor expressed by nRT neurons. Furthermore, we confirmed that nRT neurons of juvenile α3-KO mice have a deficit of gephyrin clustering at postsynaptic sites (Fig. 5A–B), as shown previously in adult mice (Studer et al., 2006). Strikingly, despite this apparent disruption of the GABAergic postsynaptic apparatus, $GABA_A$ receptor-mediated transmission was retained in the nRT (Fig. 5C). Altogether, our results suggest that concerted rescue mechanisms are activated, probably during ontogeny, to ensure the stable neuronal and network function of the thalamo-cortical circuits in α3-KO mice. This homeostatic plasticity allows for adequate thalamo-cortical network function underlying complex behaviors and their associated EEG rhythms inα3-KO mice.

Preservation of GABAergic synaptic function in the nRT

Considerable evidence *in vivo* and *in vitro* indicates that interaction with $GABA_A$ receptors containing the γ2 subunit is essential for proper clustering of gephyrin at postsynaptic sites. Thus, *in vivo* ablation of $GABA_A$ receptors by gene targeting can result in a complete loss of IPSCs and gephyrin clusters in various types of neurons (Schweizer et al., 2003, Fritschy et al., 2006, Kralic et al., 2006, Peden et al., 2007). Likewise, suppression of gephyrin expression results in a loss of $GABA_A$ receptor clusters, as shown *in vitro* (Kneussel et al., 1999, Jacob et al., 2005, Yu et al., 2007). Morphologically, the absence of α3-$GABA_A$ receptors in nRT neurons ofα3-KO mice is sufficient to prevent postsynaptic clustering of gephyrin, disclosing a mandatory interaction between the receptor and its scaffolding protein. The preservation of bicuculline-sensitive IPSCs in these cells most likely indicates that other $GABA_A$ receptor subtypes are present, possibly clustered at postsynaptic sites without interacting with gephyrin. Little information is available about the possible subunit composition of these "compensatory" receptors. Reports on $GABA_A$ receptor subunit expression in the nRT are partially controversial; aside from the α3 and γ2 subunit, these neurons might also express the α2, α5, β1, β3 and δ subunit (Fritschy and Mohler, 1995, Pirker et al., 2000, Browne et al., 2001, Huntsman and Huguenard, 2006, Studer et al., 2006). So far, no compensation by α2, α5 or δ subunit has been observed (Studer et al., 2006 and personal observations), but since an α subunit variant is required for assembly of functional $GABA_A$-receptors, the presence of low

levels of these subunits in α3-KO nRT neurons cannot be excluded. Moreover, since a targeted deletion of the α3 subunit strongly impairs the function of nRT neurons (Huntsman et al., 1999), the "compensatory" receptors are likely to contain this subunit. Finally, since the θ and ε subunit genes are frequently co-expressed withα3 (Moragues et al., 2000), and are also localized on the X-chromosome, up-regulation of these subunits in α3-KO mice is conceivable. The θ and ε subunits represent the mammalian orthologue of the avian β4 and γ4 subunit, respectively (Darlison et al., 2005). Interestingly, recombinant receptors expressing these subunits (along with α3 and β1) have a markedly enhanced GABA sensitivity (Ranna et al., 2006). Thus, if present in nRT neurons of α3-KO mice, $GABA_A$ receptors containing α2/α5, β3, andθ/ε subunits might explain preservation of large amplitude IPSCs in the absence of clustering with gephyrin.

Preservation of sIPSCs in nRT neurons of α3-KO mice suggests that a potential significance of $GABA_A$ receptor heterogeneity might be to preclude any major alterations (i.e., loss of function or "overactivity") in neuronal systems that are critical for proper brain function by allowing compensation by subtypes that are either absent or expressed at very low levels under normal, physiological conditions. The moderate phenotype of α3-KO mice stands in striking contrast with the effects of an acute pharmacological blockade of $GABA_A$ receptors. Adaptive changes preserving brain activity may be more efficient following a global loss of function than subsequent to small disturbances in the system. This aspect is illustrated by the discrepancy between the α3-KO mice, displaying no susceptibility to spike-wave seizures, and genetically epilepsy-prone rats, which lack the α3-$GABA_A$ receptors selectively in the nRT, without alteration of their expression in the cortex, and have absence-like seizures (Liu et al., 2007).

It is important to note that α3-KO mice have a global deficit of α3-$GABA_A$ receptors. The question arises whether these receptors are also replaced in other brain regions than the nRT, such as the cerebral cortex or basal forebrain in α3-KO mice. Results so far with other $GABA_A$ receptor mutant mice suggested that functional compensation can occur without replacement of $GABA_A$ receptors (Fritschy and Panzanelli, 2006). Homeostatic plasticity often involves changes in intrinsic neuronal properties that allow constant network excitability over a broad dynamic range, notably by adjusting the expression or function of various types of ion channels (reviewed in Marder and Goaillard, 2006). For instance, an adaptive increase of the potassium 'leak' conductance has been shown to preserve the integrity of excitability in the cerebellum of $GABA_A$ receptor α6-null mice, which display a complete loss of $GABA_A$-mediated tonic conductance (Brickley et al., 2001).

Significance of alterations in the sleep EEG of α3-KO mice

The retained GABAergic inhibition in the nRT may account for the lack of a robust "sleep" and "epilepsy" phenotype in α3-KO mice. With regard to sleep, we observed rather subtle alterations in the α3-KO mice. The reduced increase in power in the spindle frequency band (10–15 Hz) at the NREM-REM sleep transition in α3-KO mice is in accordance with a previous study showing that spindle activity was diminished in $GABA_A$β3-KO mice (Wisor et al., 2002), which have an impaired thalamo-cortical function (Huntsman et al., 1999). Though spindles are produced in the nRT (Fuentealba and Steriade, 2005), their synchronization is under tight control by the cortex (Steriade, 2003). Thus, the lack of α3-$GABA_A$ receptors in cortical layer VI, if not compensated for, may underlie the difference between the genotypes. During waking, α3-KO mice display an increase of EEG power density in the 11–13 Hz frequency band in the frontal derivation, which could have reflected the occurrence of spike-wave discharges. However, we did not observe any spontaneous spike-wave discharge episodes in the EEG of mutant mice, neither during baseline recordings nor following a challenge, such as sleep deprivation. Several features of REM sleep were altered in α3-KO mice, namely decreased parietal EEG power in the low theta range (4–9 Hz) associated with a faster theta-

peak frequency, as well as an increased number of longer REM sleep episodes. These changes suggest alterations in the brainstem-septo-hippocampal systems involved in the generation of theta oscillations (Vertes and Kocsis, 1997). Strikingly, basal forebrain and brainstem arousal-activating systems, which are involved in cortical activation associated with REM sleep, show a predominant distribution of α3-$GABA_A$ receptors (Gao et al., 1993, Fritschy and Mohler, 1995). Noticeably, these receptors are the main subtype expressed in several neuronal networks playing a major role in REM sleep onset and maintenance, including basal forebrain cholinergic neurons, serotonergic neurons, and noradrenergic cells of the locus coeruleus (Gao et al., 1995, Rodriguez-Pallares et al., 2001, Jones, 2005). Minor alterations in the excitability and thereby firing patterns of these neuronal populations, due to lack of α3-$GABA_A$ receptors, may underlie the subtle variations in REM sleep observed in mutant mice.

Consistent with the lack of major difference observed in EEG spectra, we found no differences in vigilance states or in locomotor activity in the home cage between WT and mutant mice. Furthermore, SD did not uncover any prominent differences between genotypes. The minor increase observed in the NREM sleep spectrum (parietal derivation) and in the REM sleep spectrum (both derivations) during the first 2 h of recovery in α3-KO mice were short lasting, which is in contrast with the robust effect induced by SD in both genotypes, waning only after 6 h recovery. The time course of recovery is in accordance with previous studies in mice (Huber et al., 2000b, Huber et al., 2000a). Moreover, in the intrahippocampal kainate model of TLE, α3-KO mice showed the same sensitivity as WT mice to this excitotoxic insult. This finding confirms that the absence of α3-$GABA_A$ receptors was functionally compensated for in the affected neuronal circuits contributing to epileptogenesis and seizure control. We have shown previously a similar compensation in α1-KO mice, which lack a large subset of $GABA_A$ receptors in hippocampal neurons, but do not exhibit any increased susceptibility to kainic acid injection (Schneider Gasser et al., 2007).

The role of α3-$GABA_A$ receptors was previously investigated using point-mutated α3(H126R) mice in which α3-$GABA_A$ receptors are diazepam-insensitive. Theα3-$GABA_A$ receptors were shown not to be critical in mediating the effects of diazepam on the sleep EEG (Kopp et al., 2003). In contrast, the anti-absence drug clonazepam has been reported to suppress thalamic oscillations via the α3-$GABA_A$ receptors (Sohal et al., 2003).

Conclusions

$GABA_A$ receptor subtypes are exquisitely tuned to regulate specific brain function and behavioral states, as demonstrated by pharmacological analysis of mice carrying point-mutations abrogating diazepam effects in selected $GABA_A$ receptors (reviewed in Rudolph and Mohler, 2004). In striking contrast to these findings, selective elimination of these receptors by gene targeting fails, in some cases, to produce a major phenotype, presumably due to the activation of compensatory mechanisms. The $GABA_A$ α1-KO mice constitute a remarkable example. Despite the loss of α1β2γ2, the most abundant receptor subtype, $GABA_A$-α1 KO mice were viable and only exhibited a mild behavioral phenotype (Sur et al., 2001, Kralic et al., 2002). Here, we show that these adaptive changes are sophisticated enough to sustain thalamo-cortical network performance underlying complex behaviors and their associated EEG rhythms inα3-KO mice. The preservation of the EEG power spectrum across the sleep-wake cycle, the lack of spike-and-waves underlying absence seizures, and the unaltered response to an excitotoxic brain lesion collectively document the effectiveness of homeostatic brain plasticity to sustain complex behavioral functions under physiological conditions and in response to a major challenge.

Abbreviations

EEG

electroencephalogram

EMG
electromyogram

GABA
gamma-aminobutyric acid

KO
knockout

NREM sleep
non rapid-eye movement sleep

nRT
reticular nucleus of the thalamus

SD
sleep deprivation

sIPSCs
spontaneous inhibitory postsynaptic currents

SWA
slow-wave activity

TLE
temporal lobe epilepsy

WT
wild-type

References

Borbély, AA.; Achermann, P. Sleep homeostasis and models of sleep regulation. In: Kryger, MH., et al., editors. Principles and Practice of Sleep Medicine. Elsevier Saunders.; Philadelphia: 2005. p. 405-417.

Bouilleret V, Loup F, Kiener T, Marescaux C, Fritschy JM. Early loss of interneurons and delayed subunit-specific changes in $GABA_A$-receptor expression in a mouse model of mesial temporal lobe epilepsy. Hippocampus 2000;10:305–324. [PubMed: 10902900]

Brickley SG, Revilla V, Cull-Candy SG, Wisden W, Farrant M. Adaptive regulation of neuronal excitability by a voltage-independent potassium conductance. Nature 2001;409:88–92. [PubMed: 11343119]

Browne SH, Kang J, Akk G, Chiang LW, Schulman H, Huguenard JR, Prince DA. Kinetic and pharmacological properties of $GABA_A$ receptors in single thalamic neurons and $GABA_A$ subunit expression. J Neurophysiol 2001;86:2312–2322. [PubMed: 11698521]

Cox CL, Huguenard JR, Prince DA. Heterogeneous axonal arborizations of rat thalamic reticular neurons in the ventrobasal nucleus. J Comp Neurol 1996;366:416–430. [PubMed: 8907356]

Cox CL, Huguenard JR, Prince DA. Nucleus reticularis neurons mediate diverse inhibitory effects in thalamus. Proc Natl Acad Sci U S A 1997;94:8854–8859. [PubMed: 9238067]

Darlison MG, Pahal I, Thode C. Consequences of the evolution of the $GABA_A$ receptor gene family. Cell Mol Neurobiol 2005;25:607–624. [PubMed: 16075381]

Domich L, Oakson G, Steriade M. Thalamic burst patterns in the naturally sleeping cat: a comparison between cortically projecting and reticularis neurones. J Physiol 1986;379:429–449. [PubMed: 3560000]

Fritschy JM, Mohler H. $GABA_A$-receptor heterogeneity in the adult rat brain: differential regional and cellular distribution of seven major subunits. J Comp Neurol 1995;359:154–194. [PubMed: 8557845]

Fritschy JM, Panzanelli P. Molecular and synaptic organization of $GABA_A$ receptors in the cerebellum: Effects of targeted subunit gene deletions. Cerebellum 2006;5:275–285. [PubMed: 17134990]

Fritschy JM, Panzanelli P, Kralic JE, Vogt KE, Sassoe-Pognetto M. Differential dependence of axo-dendritic and axo-somatic GABAergic synapses on $GABA_A$ receptors containing the α1 subunit in Purkinje cells. J Neurosci 2006;26:3245–3255. [PubMed: 16554475]

Fuentealba P, Steriade M. The reticular nucleus revisited: intrinsic and network properties of a thalamic pacemaker. Prog Neurobiol 2005;75:125–141. [PubMed: 15784303]

Gao B, Fritschy JM, Benke D, Mohler H. Neuron-specific expression of $GABA_A$-receptor subtypes: differential association of the α1- and α3-subunits with serotonergic and GABAergic neurons. Neuroscience 1993;54:881–892. [PubMed: 8393540]

Gao B, Hornung JP, Fritschy JM. Identification of distinct $GABA_A$-receptor subtypes in cholinergic and parvalbumin-positive neurons of the rat and marmoset medial septum-diagonal band complex. Neuroscience 1995;65:101–117. [PubMed: 7753393]

Huber R, Deboer T, Tobler I. Effects of sleep deprivation on sleep and sleep EEG in three mouse strains: empirical data and simulations. Brain Res 2000a;857:8–19. [PubMed: 10700548]

Huber R, Deboer T, Tobler I. Topography of EEG dynamics after sleep deprivation in mice. J Neurophysiol 2000b;84:1888–1893. [PubMed: 11024081]

Huber R, Tononi G, Cirelli C. Exploratory behavior, cortical BDNF expression, and sleep homeostasis. Sleep 2007;30:129–139. [PubMed: 17326538]

Huguenard JR, Prince DA. Clonazepam suppresses $GABA_B$-mediated inhibition in thalamic relay neurons through effects in nucleus reticularis. J Neurophysiol 1994a;71:2576–2581. [PubMed: 7931539]

Huguenard JR, Prince DA. Intrathalamic rhythmicity studied *in vitro*: nominal T-current modulation causes robust antioscillatory effects. J Neurosci 1994b;14:5485–5502. [PubMed: 8083749]

Huntsman MM, Huguenard JR. Fast IPSCs in rat thalamic reticular nucleus require the $GABA_A$ receptor β1 subunit. J Physiol 2006;572:459–475. [PubMed: 16469775]

Huntsman MM, Porcello DM, Homanics GE, DeLorey TM, Huguenard JR. Reciprocal inhibitory connections and network synchrony in the mammalian thalamus. Science 1999;283:541–543. [PubMed: 9915702]

Jacob TC, Bogdanov YD, Magnus C, Saliba RS, Kittler JT, Haydon PG, Moss SJ. Gephyrin regulates the cell surface dynamics of synaptic $GABA_A$ receptors. J Neurosci 2005;25:10469–10478. [PubMed: 16280585]

Jones, BE. Basic mechanisms of sleep-wake states. In: Kryger, MH., et al., editors. Principles and Practice of Sleep Medicine. Elsevier Saunders; Philadelphia: 2005. p. 136-153.

Jones EG. Thalamic circuitry and thalamocortical synchrony. Philos Trans R Soc Lond B Biol Sci 2002;357:1659–1673. [PubMed: 12626002]

Kneussel M, Brandstatter JH, Laube B, Stahl S, Muller U, Betz H. Loss of postsynaptic $GABA_A$ receptor clustering in gephyrin-deficient mice. J Neurosci 1999;19:9289–9297. [PubMed: 10531433]

Kopp C, Rudolph U, Keist R, Tobler I. Diazepam-induced changes on sleep and the EEG spectrum in mice: role of the alpha3-$GABA_A$ receptor subtype. Eur J Neurosci 2003;17:2226–2230. [PubMed: 12786990]

Kralic JE, Korpi ER, O'Buckley TK, Homanics GE, Morrow AL. Molecular and pharmacological characterization of $GABA_A$ receptor α1 subunit knockout mice. J Pharmacol Exp Ther 2002;302:1037–1045. [PubMed: 12183661]

Kralic JE, Ledergerber DA, Fritschy JM. Disruption of the neurogenic potential of the dentate gyrus in a mouse model of temporal lobe epilepsy with focal seizures. Eur J Neurosci 2005;22:1916–1927. [PubMed: 16262631]

Kralic JE, Sidler C, Parpan F, Homanics GE, Morrow AL, Fritschy JM. Compensatory alteration of inhibitory synaptic circuits in cerebellum and thalamus of gamma-aminobutyric acid type A receptor α1 subunit knockout mice. J Comp Neurol 2006;495:408–421. [PubMed: 16485284]

Liu XB, Coble J, van Luijtelaar G, Jones EG. Reticular nucleus-specific changes in α3 subunit protein at GABA synapses in genetically epilepsy-prone rats. Proc Natl Acad Sci U S A 2007;104:12512–12517. [PubMed: 17630284]

Liu XB, Jones EG. Predominance of corticothalamic synaptic inputs to thalamic reticular nucleus neurons in the rat. J Comp Neurol 1999;414:67–79. [PubMed: 10494079]

Llinas RR, Steriade M. Bursting of thalamic neurons and states of vigilance. J Neurophysiol 2006;95:3297–3308. [PubMed: 16554502]

Marder E, Goaillard JM. Variability, compensation and homeostasis in neuron and network function. Nat Rev Neurosci 2006;7:563–574. [PubMed: 16791145]

Moragues N, Ciofi P, Lafon P, Odessa MF, Tramu G, Garret M. cDNA cloning and expression of a gamma-aminobutyric acid A receptor ε-subunit in rat brain. Eur J Neurosci 2000;12:4318–4330. [PubMed: 11122342]

Peden DR, Petitjean CM, Herd MB, Durakoglugil M, Rosahl TW, Wafford K, Homanics GE, Belelli D, Fritschy JM, Lambert JJ. Developmental maturation of synaptic and extrasynaptic $GABA_A$ receptors in mouse thalamic ventrobasal neurones. J Physiol 2008;586:965–987. [PubMed: 18063661]

Pinault D. The thalamic reticular nucleus: structure, function and concept. Brain Res Brain Res Rev 2004;46:1–31. [PubMed: 15297152]

Pirker S, Schwarzer C, Wieselthaler A, Sieghart W, Sperk G. $GABA_A$ receptors: immunocytochemical distribution of 13 subunits in the adult rat brain. Neuroscience 2000;101:815–850. [PubMed: 11113332]

Ranna M, Sinkkonen ST, Moykkynen T, Uusi-Oukari M, Korpi ER. Impact of ε and θ subunits on pharmacological properties of α3β1 $GABA_A$ receptors expressed in *Xenopus* oocytes. BMC Pharmacol 2006;6:1. [PubMed: 16412217]

Rodriguez-Pallares J, Caruncho HJ, Lopez-Real A, Wojcik S, Guerra MJ, Labandeira-Garcia JL. Rat brain cholinergic, dopaminergic, noradrenergic and serotonergic neurons express $GABA_A$ receptors derived from the α3 subunit. Receptors Channels 2001;7:471–478. [PubMed: 11918349]

Rudolph U, Mohler H. Analysis of $GABA_A$ receptor function and dissection of the pharmacology of benzodiazepines and general anesthetics through mouse genetics. Annu Rev Pharmacol Toxicol 2004;44:475–498. [PubMed: 14744255]

Rudolph U, Mohler H. GABA-based therapeutic approaches: $GABA_A$ receptor subtype functions. Curr Opin Pharmacol 2006;6:18–23. [PubMed: 16376150]

Schneider Gasser EM, Duveau V, Prenosil GA, Fritschy JM. Reorganizationof GABAergic circuits maintains $GABA_A$ receptor-mediated transmission onto CA1 interneurons in α1-subunit-null mice. Eur J Neurosci 2007;25:3287–3304. [PubMed: 17552997]

Schweizer C, Balsiger S, Bluethmann H, Mansuy IM, Fritschy JM, Mohler H, Luscher B. The γ2 subunit of $GABA_A$ receptors is required for maintenance of receptors at mature synapses. Mol Cell Neurosci 2003;24:442–450. [PubMed: 14572465]

Sohal VS, Huguenard JR. Inhibitory interconnections control burst pattern and emergent network synchrony in reticular thalamus. J Neurosci 2003;23:8978–8988. [PubMed: 14523100]

Sohal VS, Huntsman MM, Huguenard JR. Reciprocal inhibitory connections regulate the spatiotemporal properties of intrathalamic oscillations. J Neurosci 2000;20:1735–1745. [PubMed: 10684875]

Sohal VS, Keist R, Rudolph U, Huguenard JR. Dynamic $GABA_A$ receptor subtype-specific modulation of the synchrony and duration of thalamic oscillations. J Neurosci 2003;23:3649–3657. [PubMed: 12736336]

Steriade M. The corticothalamic system in sleep. Front Biosci 2003;8:d878–899. [PubMed: 12700074]

Steriade M. Sleep, epilepsy and thalamic reticular inhibitory neurons. Trends Neurosci 2005;28:317–324. [PubMed: 15927688]

Steriade M. Grouping of brain rhythms in corticothalamic systems. Neuroscience 2006;137:1087–1106. [PubMed: 16343791]

Steriade M, Domich L, Oakson G. Reticularis thalami neurons revisited: activity changes during shifts in states of vigilance. J Neurosci 1986;6:68–81. [PubMed: 3944624]

Steriade M, McCormick DA, Sejnowski TJ. Thalamocortical oscillations in the sleeping and aroused brain. Science 1993;262:679–685. [PubMed: 8235588]

Studer R, von Boehmer L, Haenggi T, Schweizer C, Benke D, Rudolph U, Fritschy JM. Alteration of GABAergic synapses and gephyrin clusters in the thalamic reticular nucleus of $GABA_A$ receptor α3 subunit-null mice. Eur J Neurosci 2006;24:1307–1315. [PubMed: 16987218]

Sur C, Wafford KA, Reynolds DS, Hadingham KL, Bromidge F, Macaulay A, Collinson N, O'Meara G, Howell O, Newman R, Myers J, Atack JR, Dawson GR, McKernan RM, Whiting PJ, Rosahl TW. Loss of the major $GABA_A$ receptor subtype in the brain is not lethal in mice. J Neurosci 2001;21:3409–3418. [PubMed: 11331371]

Timofeev I, Steriade M. Neocortical seizures: initiation, development and cessation. Neuroscience 2004;123:299–336. [PubMed: 14698741]

Tobler I, Deboer T, Fischer M. Sleep and sleep regulation in normal and prion protein-deficient mice. J Neurosci 1997;17:1869–1879. [PubMed: 9030645]

Tobler I, Gaus SE, Deboer T, Achermann P, Fischer M, Rulicke T, Moser M, Oesch B, McBride PA, Manson JC. Altered circadian activity rhythms and sleep in mice devoid of prion protein. Nature 1996;380:639–642. [PubMed: 8602267]

Valatx JL, Bugat R. Genetic factors as determinants of the waking-sleep cycle in the mouse. Brain Res 1974;69:315–330. [PubMed: 4362814]

Vertes RP, Kocsis B. Brainstem-diencephalo-septohippocampal systems controlling the theta rhythm of the hippocampus. Neuroscience 1997;81:893–926. [PubMed: 9330355]

von Krosigk M, Bal T, McCormick DA. Cellular mechanisms of a synchronized oscillation in the thalamus. Science 1993;261:361–364. [PubMed: 8392750]

Vyazovskiy VV, Achermann P, Borbely AA, Tobler I. The dynamics of spindles and EEG slow-wave activity in NREM sleep in mice. Arch Ital Biol 2004;142:511–523. [PubMed: 15493552]

Watanabe M, Fukaya M, Sakimura K, Manabe T, Mishina M, Inoue Y. Selective scarcity of NMDA receptor channel subunits in the stratum lucidum (mossy fibre-recipient layer) of the mouse hippocampal CA3 subfield. Eur J Neurosci 1998;10:478–487. [PubMed: 9749710]

Wisden W, Laurie DJ, Monyer H, Seeburg PH. The distribution of 13 $GABA_A$ receptor subunit mRNAs in the rat brain. I. Telencephalon, diencephalon, mesencephalon. J Neurosci 1992;12:1040–1062. [PubMed: 1312131]

Wisden W, Morris BJ, Darlison MG, Hunt SP, Barnard EA. Distinct $GABA_A$ receptor alpha subunit mRNAs show differential patterns of expression in bovine brain. Neuron 1988;1:937–947. [PubMed: 2856089]

Wisor JP, DeLorey TM, Homanics GE, Edgar DM. Sleep states and sleep electroencephalographic spectral power in mice lacking the α3 subunit of the $GABA_A$ receptor. Brain Res 2002;955:221–228. [PubMed: 12419540]

Yee BK, Keist R, von Boehmer L, Studer R, Benke D, Hagenbuch N, Dong Y, Malenka RC, Fritschy JM, Bluethmann H, Feldon J, Mohler H, Rudolph U. A schizophrenia-related sensorimotor deficit links α3-containing $GABA_A$ receptors to a dopamine hyperfunction. Proc Natl Acad Sci U S A 2005;102:17154–17159. [PubMed: 16284244]

Yu W, Jiang M, Miralles CP, Li RW, Chen G, de Blas AL. Gephyrin clustering is required for the stability of GABAergic synapses. Mol Cell Neurosci 2007;36:484–500. [PubMed: 17916433]

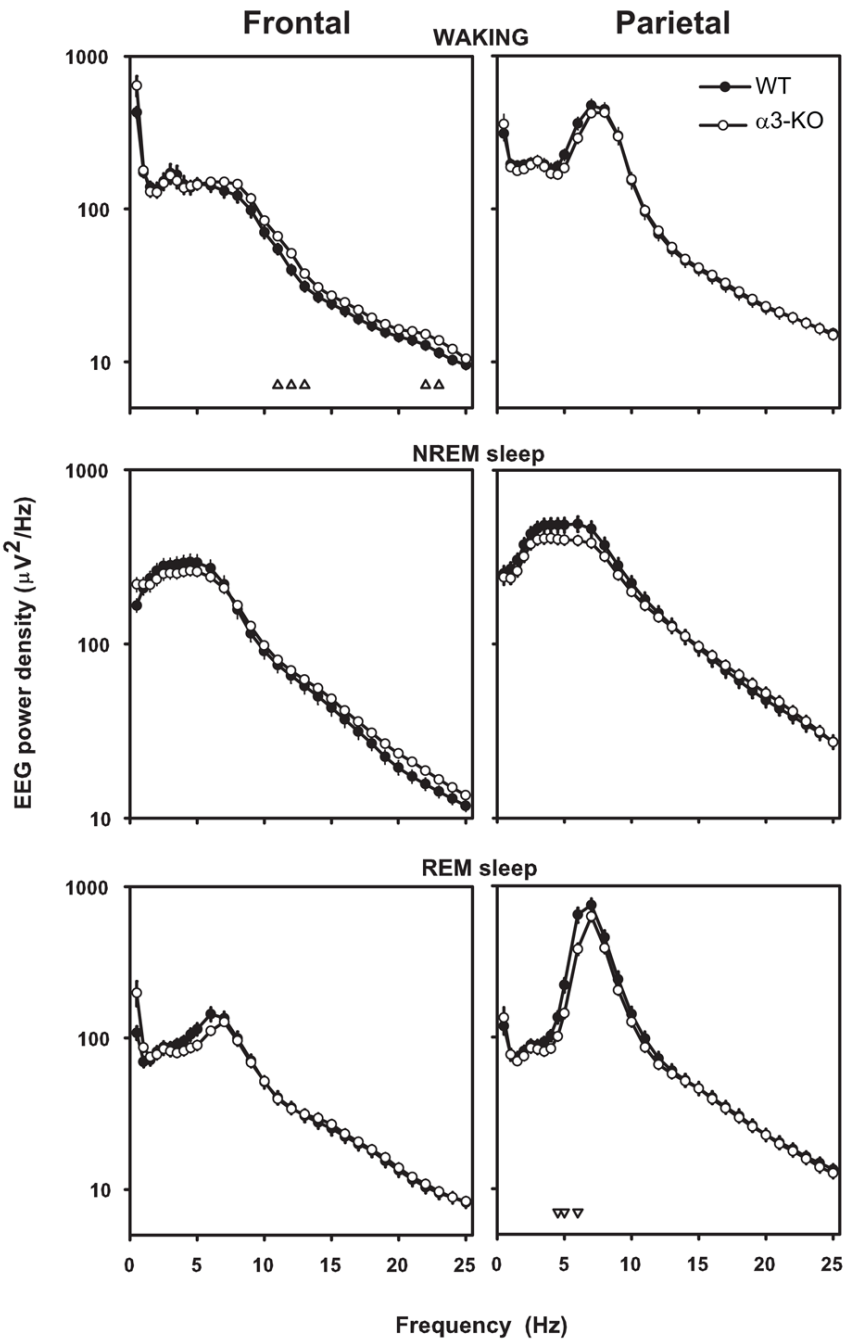

Figure 1. EEG power density in the three vigilance states during the 12-h baseline light period

Curves represent logarithmic mean values of absolute power densities (n = 11 WT; n = 12 α3-KO mice) for the frontal and parietal EEG in waking, NREM sleep and REM sleep. Values are plotted at the upper limit of each bin. Triangles below the curves indicate frequency bins differing significantly between genotypes and their orientation the direction of the difference (one-way ANOVA factor 'genotype'; $p < 0.05$ *post-hoc* unpaired *t*-test).

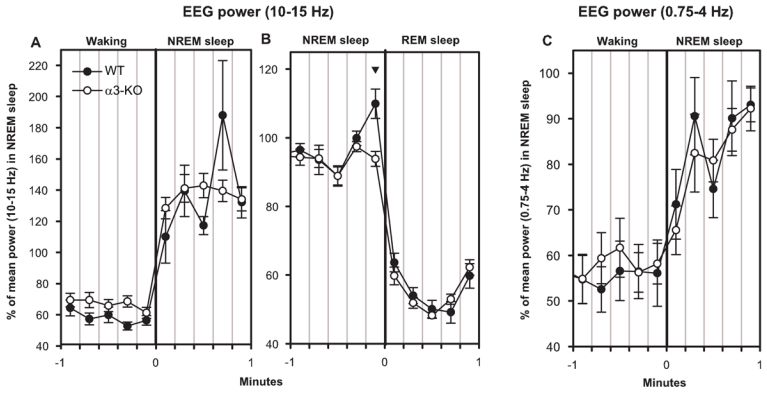

Figure 2.

Time-course of EEG power density in the 10–15 Hz frequency band (panel A and B) and 0.75–4 Hz band (C) for 1 min before and 1 min after transitions from waking to NREM sleep (A and C) and NREM sleep to REM sleep (B) in the frontal derivation. Mean values (n = 11 WT; n = 12 α3-KO mice) are expressed as percentage of mean power density in the corresponding frequency band in NREM sleep during the 12-h baseline light period. Triangle indicates a 12-s epoch which differed between α3-KO (open circles) and WT (black circles) mice ($p<0.05$; *post-hoc* unpaired *t*-test after significant two-way ANOVA with factors ‘genotype’ and ‘epoch’).

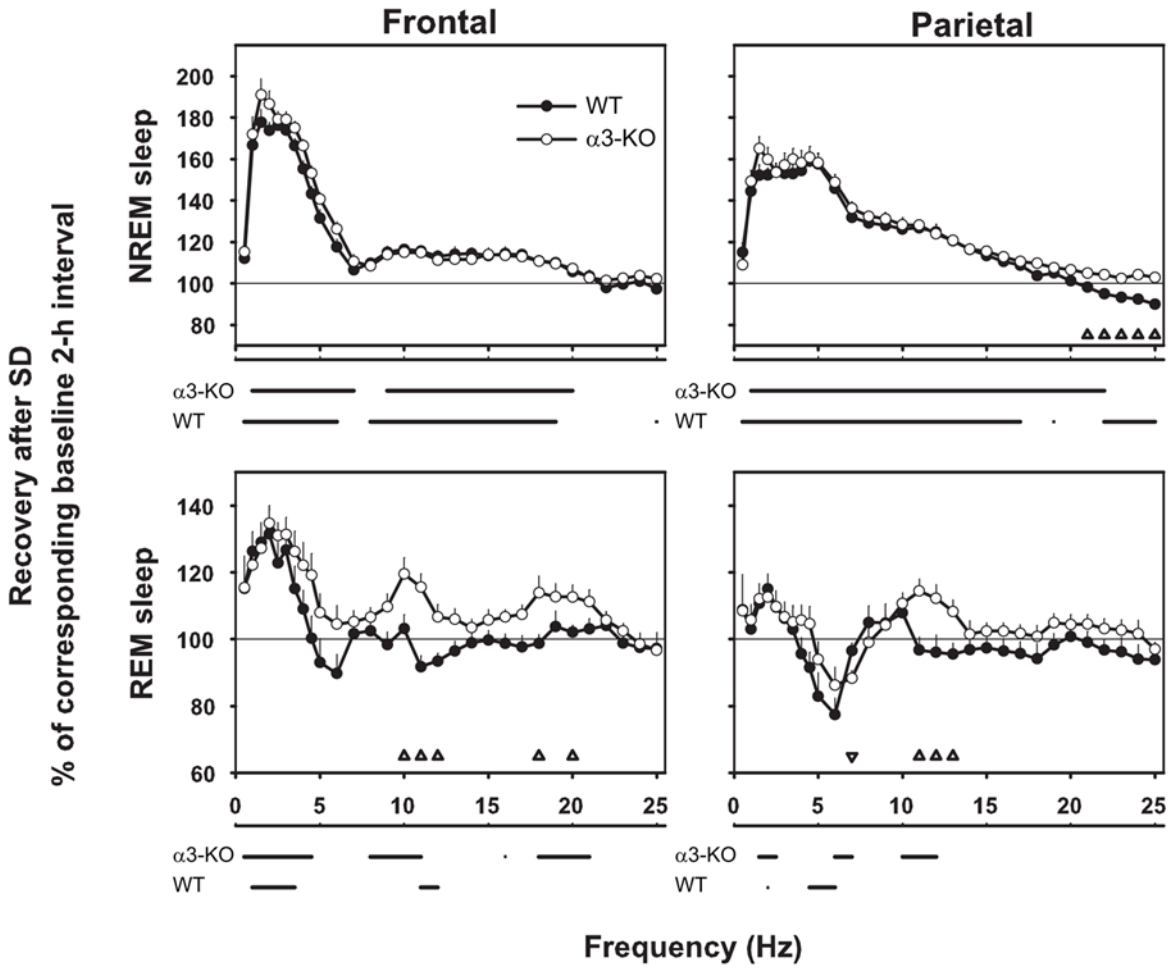

Figure 3. EEG power density in NREM sleep and REM sleep computed for the first 2-h interval during recovery from 6 h sleep deprivation (SD)

Mean values (n = 11 WT; n = 12 α3-KO mice) are expressed for each frequency bin as percentage of the same bin during the corresponding baseline interval, separately for the frontal and the parietal EEG. Horizontal lines below the curves show the significances for the effect of SD for each genotype (rANOVA factor 'day'; $p<0.05$ *post-hoc* paired *t*-test) Triangles indicate frequency bins differing between genotypes and their orientation the direction of the difference (one-way ANOVA factor 'genotype'; $p < 0.05$, unpaired *t*-test).

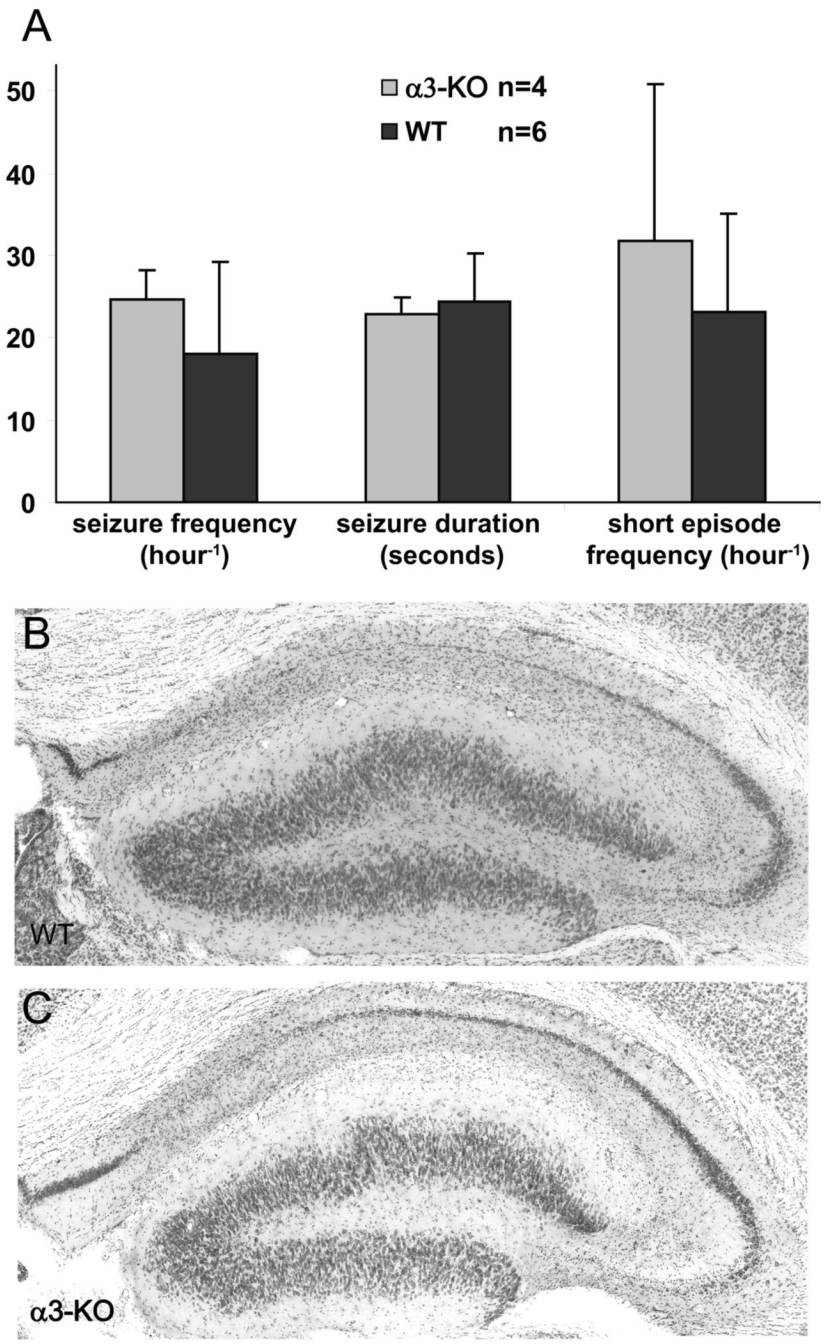

Figure 4.

A) Average (mean ± SD) frequency and duration of seizures and average frequency of short ictal episodes in WT (n=4) and α3-KO mice (n=6), as recorded by EEG 28 days after intrahippocampal kainic acid injection. Statistical analysis (unpaired *t*-test) revealed no significant differences among genotypes. B–C) Histopathological changes induced by kainic acid injection in the dorsal hippocampus, as seen by Cresyl violet staining. Sections were prepared after completion of EEG recordings. The extent of neurodegeneration in CA1, CA3, and hilus, and the dispersion of granule cells in the dentate gyrus, are similar in WT (B) and in mutant (C) mice. Scale bar, 200 μm.

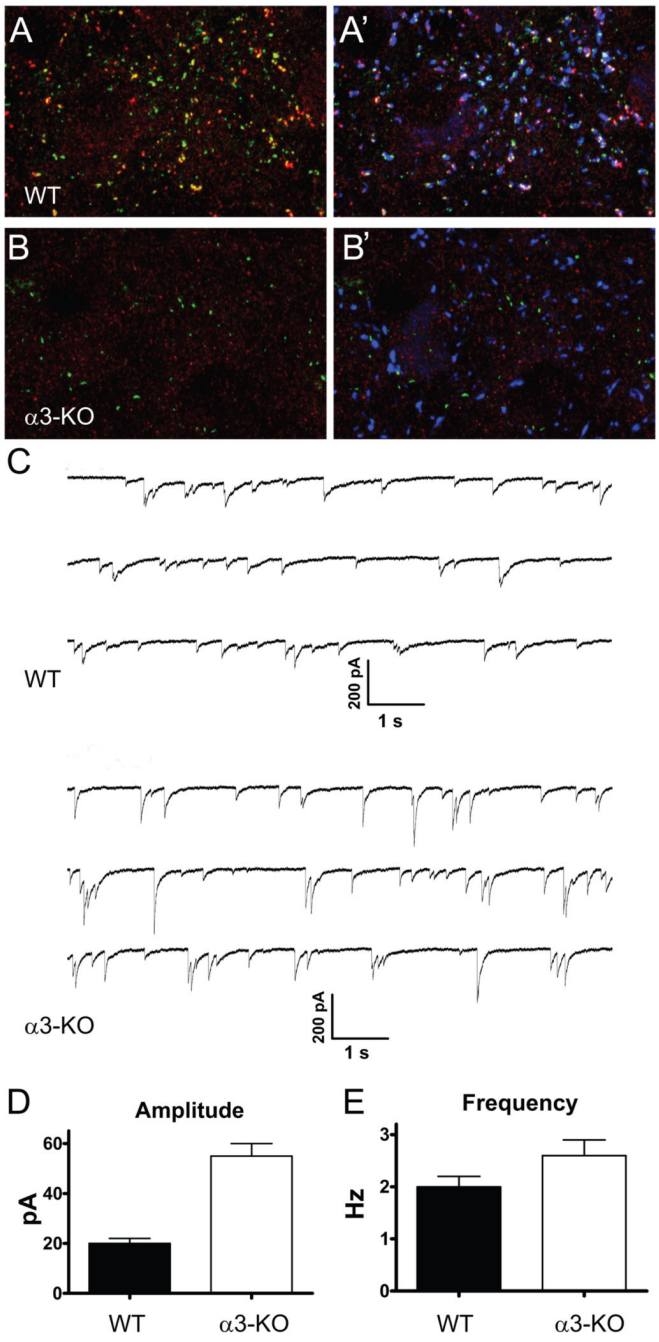

Figure 5.

A–B) Loss of $GABA_A$ receptor α3 subunit (red) and gephyrin (green) clusters in α3-KO mice at the age of P15, as visualized by immunofluorescence staining. In sections from WT mice, these clusters are extensively co-localized (yellow hue in A) and apposed to presynaptic GABAergic terminals (stained for VIAAT, blue, in A Figure 1. EEG power density in the three vigilance states during the 12-h baseline light period.

Curves represent logarithmic mean values of absolute power densities (n = 11 WT; n = 12 α3-KO mice) for the frontal and parietal EEG in waking, NREM sleep and REM sleep. Values are plotted at the upper limit of each bin. Triangles below the curves indicate frequency bins

differing significantly between genotypes and their orientation the direction of the difference (one-way ANOVA factor ‘genotype’; $p < 0.05$ *post-hoc* unpaired *t*-test).

Table 1

Vigilance states in α3-KO and WT mice during baseline and recovery after 6 h sleep deprivation

	WT		α3-KO	
	Baseline	**Recovery**	**Baseline**	**Recovery**
WAKING				
Light	328.6 (13.1)		329.4 (8.3)	
Dark	459.8 (10.9)	406.4 (10.6)	410.0 (9.8)	380.6 (8.4)
24 h	758.4 (18.3)		739.4 (14.3)	
Rec 7–12h		141.5 (6.4)		140.3 (2.9)
NREM Sleep				
Light	304.3 (12.5)		299.1 (6.9)	
Dark	229.4 (10.4)	247.1 (10.0)	245.8 (7.0)	262.4 (7.8)
24 h	533.7 (18.2)		544.9 (11.7)	
Rec 7–12h		170.5 (5.0)		170.2 (3.2)
REM Sleep				
Light	87.1 (2.5)		91.5 (3.3)	
Dark	60.7 (2.6)	66.5 (3.4)	64.2 (3.5)	77.0 (2.6)
24 h	147.9 (3.8)		155.7 (4.7)	
Rec 7–12h		48.0 (2.6)		49.5 (2.1)

The amount of time spent in waking, NREM sleep and REM sleep expressed in minutes. Mean values (± SEM; n = 12 α3-KO mice *versus* n = 11 WT mice) are shown for the subdivided baseline (12 h light and dark phases), the entire 24 h baseline, and for recovery after 6 h sleep deprivation (hours 7–12 of the recovery (Rec) 12 h light phase). Comparisons between genotypes were not significant for any variable (unpaired *t*-test).